

ESTIMATING THE DYNAMIC RANGE OF MUSIC SIGNALS VIA RANDOM SUBSAMPLING*

Pietro Coretto
Università di Salerno, Italy
pcoretto@unisa.it

Francesco Giordano
Università di Salerno, Italy
giordano@unisa.it

Version: Tuesday 4th March, 2025, 10:29

Abstract. The dynamic range is an important parameter which measures the spread of sound power. There are various descriptive measures of sound power, none of which has strong statistical foundations. We start from a general non-parametric model for sound waves composed by a smooth regression function plus a stochastic process belonging to a fairly rich family. The stochastic term has the role to catch transient energy so that the distribution of its variance is considered for measuring the dynamic range. We develop a rate-optimal kernel estimator to recover the unobservable stochastic component. The distribution of its variance is approximated by a consistent random subsampling method that is able to cope with the massive size of the typical dataset. Based on the latter, we propose a dynamic range statistic that shows remarkable performance.

Keywords: random subsampling, nonparametric regression, music data, dynamic range.

AMS classification: 97M80 (primary); 62M10, 62G08, 62G09, 60G35 (secondary)

1 Introduction

Music signals have a complex dynamic structure with interesting statistical properties. A music signal is the sum of periodic components plus transient components that determine changes from one dynamic level to another. The term “transients” refers to sharp changes in acoustic energy. Transients are of huge interest for several reasons. While it is relatively easier to record, transfer and reproduce soft changes, transients are much harder to catch, and they mainly contribute to the difference between recorded vs live sounds. Most recording and listening medium have to somehow compress acoustic energy variations, and

*We thank Bob Katz and Earl Vickers (both members of the Audio Engineering Society) for the precious feedback on some of the idea contained in the paper. The authors gratefully acknowledge support from the University of Salerno grant program “Finanziamento di attrezzature scientifiche e di supporto per i Dipartimenti e i Centri Interdipartimentali - prot. ASSA098434, 2009”.

this causes that transient peaks are strongly reduced with respect to average signal level. The latter is also known as “dynamic range compression”. The dynamic range (DR) of a signal is the spread of acoustic power. Loss of DR along the recording-to-play back chain translates into a loss of audio fidelity. While DR is a well established technical concept, there is no consensus on how to define it and how to measure it, at least in the field of music signals. Practitioners in the audio industry use to measure the DR based on various descriptive statistics for which little is known in terms of their statistical properties [Boley et al., 2010; Ballou, 2005]. In this paper we propose a measure of DR that is based on statistical methods with proven properties.

The main idea of the paper is that the dynamic structure of a music signal is characterized by the energy produced by transient dynamic so that the DR is measured by looking at the distribution of transient power. We propose a nonparametric model composed by two elements: (i) a periodic component consisting in a smooth deterministic function; (ii) a stochastic component representing transients. In this framework transient power is given by the variance of the stochastic component. By consistently estimating the distribution of the variance of the stochastic component, we obtain the distribution of the power expressed by the stochastic component which, in turn, is the basis for constructing our DR statistic.

The idea of decomposing the music signal into a deterministic function of time plus a stochastic component is not new [see Beran, 2004b; Benson, 2004, and references therein]. However, it is usually assumed that the stochastic term of this decomposition belongs to a class of linear processes. The first novelty in this paper is that we propose a decomposition where the stochastic term is an α -mixing process, and this assumption allows to accommodate transient structures beyond those allowed by linear processes. The stochastic component is obtained by filtering out the smooth component of the signal, and this is approximated with kernel regression methods. Optimality of kernel regression methods with serial dependence in the error term has been studied in Altman [1990]. However the latter contribution sticks on the assumptions that: (i) the error term belongs to the class of linear processes; (ii) serial correlations of this process are known. The second contribution of this work is that we develop upon Altman’s seminal paper obtaining a rate optimal kernel estimator without assuming linearity and knowledge of the correlation structure of the stochastic term. Approximation of the distribution of the variance of the stochastic component of the signal is done by a subsampling scheme inspired to that developed by Politis and Romano [1994] and Politis et al. [2001]. The standard subsampling requires to compute the variance of the the stochastic component on the entire sample, which in turn means that we need to compute the kernel estimate of the smooth component over the entire sample. The latter is unfeasible given the astronomically large nature of the typical sample size. A third contribution of the paper is that we propose a consistent random subsampling scheme that does only require computations on single subsamples. We use the quantiles of the variance distribution of the stochastic component to build our DR statistic. Our DR statistic, when applied on real sound waves, is able to detect small differences in dynamic levels. We provide an extensive empirical study where we show that: (i) subtle dynamic contrasts are successfully captured by the stochastic component; (ii) the statistical method proposed here provides a dynamic measure that outperforms those based on descriptive statistics.

The paper is organized as follows: in Section 2 we review technical concepts related the to

physic of sound, in Section 3 we illustrate our modelling strategy, in Section 4 we develop the main statistical tools, in Section 5 we propose our dynamic range statistic, in Section 6 we show empirical results based on real data, while in Section 7 we set some final remarks. All proofs of statements are given in the appendix.

2 Background concepts: sound waves, power and dynamic

A sound source radiates acoustic energy and this results in a sound pressure which is captured by the hearing system. Rate of change of acoustic energy is equal to acoustic power, also called sound power. Let $x(t)$ be a continuous time waveform. At time t the value $x(t)$ is equal to the amplitude of an audio stimuli. In general for a time varying waveform power changes over time. For a continuous waveform $x(t)$ taking values on the time interval $T_1 \leq t \leq T_2$, such that $\int_{T_1}^{T_2} x(t)dt = 0$, the power is given by

$$P_{x(t)}^{RMS} = C \sqrt{\frac{1}{T_2 - T_1} \int_{T_1}^{T_2} x(t)^2 dt} \quad (2.1)$$

provided that the integral above exists. C is an appropriate scaling constant that depends on the measurement unit. Equation (2.1) defines the so called root mean square (RMS) power. Expression (2.1) tells us that the power expressed by a waveform is determined by the average magnitude of the wave swings around its average level. In other words the equation (2.1) reminds us the concept of standard deviation. In acoustics the sound power is conveniently expressed on log-scale because this approximates the psychological and physiological responses of humans to acoustic stimuli [see Ballou, 2005; Crocker, 1998]. We conveniently express sound power relatively to a reference value set as baseline obtaining decibels of sound pressure levels,

$$\text{dB}_{\text{SPL}} = 20 \log_{10} \frac{P^{RMS} \text{ Pa}}{20 \mu\text{Pa}},$$

with Pa=Pascal unit. The denominator of dB_{SPL} defines the 0dB_{SPL} reference point under which almost no humans can hear. For instance 40dB_{SPL} is the sound power produced by a buzzing mosquito around the head, $180\text{dB}_{\text{SPL}}$ is the sound power produced by a jet engine at one meter.

The sound wave $x(t)$ can be recorded and stored by means of analog and/or digital processes. In the digital world $x(t)$ is represented numerically by sampling and quantizing the analog version of $x(t)$. The sampling scheme underlying the so called Compact Disc Digital Audio (CDDA), patented by Philips and Sony in the '80s, is called Pulse Code Modulation (PCM). In PCM coding a voltage signal $x(t)$ is sampled as a sequence of integer values proportional to the level of $x(t)$ at equally spaced times t_0, t_1, \dots . The CDDA is based on PCM coding with sampling frequency equal to 44.1KHz and bit precision equal to 16bits. The sampling frequency at 44.1KHz allows to capture harmonic contents up to 22KHz (by Nyquist theorem), which is slightly above the upper limit of the human hearing system. The 16bits precision means that the signal $x(t)$ is quantized using 2^{16} integer values. The quantization process introduces rounding errors also known as quantization noise or quantization error (QE) [see Bennett, 1948; Perez-Alcazar and

[Santos, 2002]. Each operation in the PCM domain increases the energy of the quantization noise, which is considered as the main source of digital noise. Based on the PCM samples $\{x_0, x_2, \dots, x_T\}$, and under strong conditions on the structure of the underlying $x(t)$, the RMS power can be approximated by

$$P_T^{RMS} = \sqrt{\frac{1}{T+1} \sum_{t=0}^T x_t^2}. \quad (2.2)$$

P_T^{RMS} is the sample analog of (2.1) provided that the average of sample values is approximately equal to zero (which is always the case for music signals). Given a reference waveform one can construct a PCM analog of dB_{SPL} by defining ‘‘Full Scale Decibels’’

$$\text{dBFS} = 20 \log_{10} \frac{P_T^{RMS}}{P_0} \quad (2.3)$$

where P_0 is the RMS power of a reference waveform such that its power doesn’t depend on T , and its range covers the range of PCM quantization levels. Usually the reference waveform is either set to a sine wave or a square wave. If the PCM samples are scaled onto the interval $[-1,1]$, $P_0 = 1/\sqrt{2}$ with reference to a sine wave, and $P_0 = 1$ with reference to a square wave. For the sake of simplifying calculations we set $P_0 = 1$ in this paper, even though $1/\sqrt{2}$ is more popular. dBFS is commonly considered as DR measure because it measures the spread of the sound power with respect to a reference full scale signal.

Notice that the dBFS definition above depends on T because of P_T^{RMS} . For most real-world signal power changes strongly over time. In Figure 1 we report a piece of sound extracted from the left channel of the song ‘‘In the Flesh?’’ by Pink Floyd. The wave above is centered (vertical line) around 20.395s from the beginning and it is 980ms long. The plot below only reports the first half of the plot above. At the center point (20.39sec) a sharp transition happens. If we would look at the plot with statistics in mind we would say that we have a time series with a tremendous structural break, there are two regimes with completely different dynamic structures. The samples reported are only a tiny fraction of the entire song, and if we would look at the entire wave we would have seen several of such breaks and changes. We learn two things: (i) sound power of music signals can change tremendously over time; (ii) the sound power we measure depends on T , that is the time horizon on which we integrate the squared magnitude of the signal.

In the audio engineering community the practical approach is to time-window the signal and compute average power across windows, then several forms of DR statistics are computed [see Ballou, 2005] based on dBFS. In practice one chooses a T , then splits the PCM sequence into blocks of T samples allowing a certain number h of overlapping samples between blocks, let $\overline{P_T^{RMS}}$ be the average of P_T^{RMS} values computed on each block, finally a simple DR measure, that we call ‘‘sequential DR’’, is computed as

$$\text{DRS} = -20 \log_{10} \frac{\overline{P_T^{RMS}}}{x_{\text{peak}}}, \quad (2.4)$$

where x_{peak} is the observed maximum absolute value. The role of x_{peak} is to scale the DR measure so that it does not depend on the range of PCM values covered by the recorded signal. In fact, for good technical reasons, it is advised that quantized signal stays well

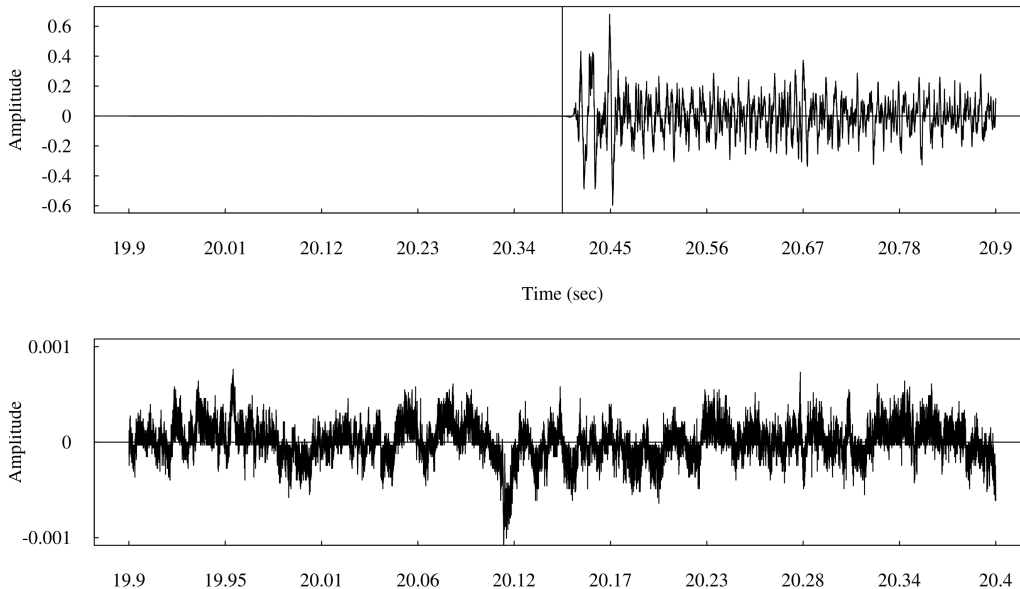


Figure 1: Waveform of the left channel for the song “*In the Flesh?*” from “*The Wall*” album by Pink Floyd remastered by Mobile Fidelity Sound Lab (catalog no. UDCD 2-537). The plot above captures 980ms of music centered at 20.39524s from the beginning of the track. The plot below reports the first half of the wave above.

within the range of the PCM quantization levels available. This is called “headroom”. The time windowing can be further sophisticated by introducing some of the window function used in spectral analysis. $DRS=10$ means that on average the RMS power is 10dBFS below the maximum signal amplitude. Even though DRS numbers are easily interpretable, the statistical motivation is weak. Since the blocks are sequential, T and h determine the blocks uniquely regardless the structure of the signal at hand. For music signals, a common default value is a block length of 50ms with 25% to 50% of overlapping samples. This is because 50ms will contain an entire cycle of the lowest frequency detectable by the average human hearing (that is 20Hz). Boley et al. [2010] reports various qualitative justifications and recommendations for various window lengths based on physical arguments. To our knowledge there is no literature that systematically investigates the effects of windows type and length for real world music signals. In the case of Figure 1 what happens if T, h are picked so that a power measurements is taken in the middle of the transition? The second issue is whether the average $\overline{P^{RMS}_T}$ is a good measure of the sound power distribution to express the DR concept. Certainly the descriptive nature of the DRS statistics and the lack of a stochastic framework does not allow to make inference and judge numbers consistently.

3 Statistical Modelling

The German theoretical physicist Herman Von Helmholtz (1885) discovered that within small time intervals sound signals produced by instruments are periodic and hence representable as sums of periodic functions of time. Based on the theory of vibrating strings, theoretical physics describes a sound wave produced by acoustic instruments as a function

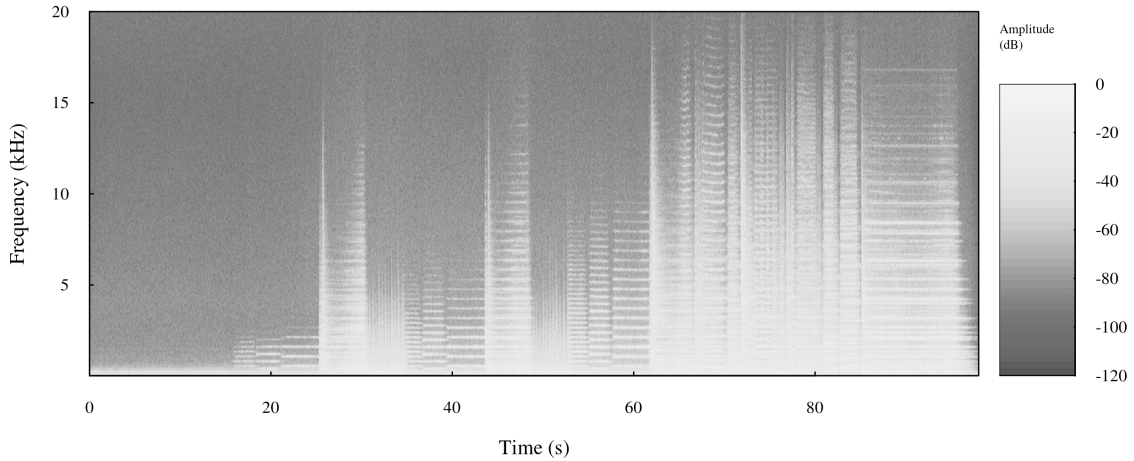


Figure 2: Spectrogram of the right channel of the opening fanfare of “Also Sprach Zarathustra” (Op. 30) by Richard Strauss, performed by Vienna Philharmonic Orchestra conducted by Herbert von Karajan (Decca, 1959). The power spectra values are expressed in dBFS scale and coded as colors ranging from black (low energy) to white (high energy).

of the form

$$y(t) = \sum_{j=1}^J A_j \cos(\phi_j + 2\pi jft), \quad (3.1)$$

where t represents units of time (usually seconds), f is the fundamental frequency expressed in Hz (cycles per second), the terms of the sum in (3.1) are referred as harmonic components each one appearing with amplitude (intensity) A_j and phase angle ϕ_j . For a given f , the particular combination of the set of parameters $\{A_j, \phi_j; j = 1, 2, \dots, J\}$ defines the particular tune of an instruments. [Risset and Mathews \[1969\]](#) studied the local behavior of the harmonic components of sound signals from instruments playing simple tunes. They discovered that the intensity of the harmonic components varied strongly over time which means that the implied signals were not really representable by (3.1) even for short time lengths. They also showed how in reality instruments have a spectral energy distribution that is not discrete as (3.1) would suggest. [Irizarry \[2001\]](#) presented examples of time windowed spectrogram for single tunes of acoustic instruments. He showed that, even though locally the signals are approximately periodic, the harmonic components are time-varying. Figure 2 reports the spectrogram of famous fanfare. A spectrogram is a periodogram computed on rolling time-windows, with periodogram values expressed in dBFS. The spectrogram of Figure 2 has been computed using a Hanning window function, each time window takes about 50ms of music, the overlap between two successive time-windows is about 25%, which is a common strategy in sound analysis [[Thomson, 1982](#)]. At a particular time-frequency point the spectrogram tell us the acoustic energy in a neighbourhood of that point, going from white (high energy) to black (low energy). This is a particularly dynamic piece of sound, the orchestra plays a soft opening followed by a series of transients at full blast with varying decay-time. Figure 2 reveals that most acoustic energy, as expected, is localized below 1KHz. There are several changes in the spectral distribution over time. However, if we fix the attention at a particular time point there are peaks localized in several frequency bands, but there is a continuum of energy

spread between peaks. From this example it is clear that while the periodic component is strong, there is a relevant continuous component. Moreover, there are several transients that change the acoustic energy sharply, and during those transients the acoustic energy is spread continuously over a wide frequency bandwidth. This shows how transient changes are strongly characterized by a continuous spectral component.

Our model for the PCM samples is as follows. Let $\{Y_t\}_{t \in \mathbb{Z}}$ be a sequence such that

$$Y_t = s(t) + \varepsilon_t, \quad (3.2)$$

where $s(\cdot)$ is a real valued smooth function of time, and $\{\varepsilon_t\}_{t \in \mathbb{Z}}$ is a real valued stochastic process. The equation (3.2) is by no means interpretable as a Tukey-kind signal plus noise decomposition. The observable (recorded) sound wave Y_t deviates from $s(t)$ because of several factors: (i) sonic features not explained in (3.1); (ii) transient changes in acoustic energy; (iii) several sources of noise injected in the recording path. We call the process $\{\varepsilon_t\}_{t \in \mathbb{Z}}$ the “*stochastic sound wave*” (SSW). Our model is completed by the following assumptions.

A 1. The function $s(t)$ has a continuous second derivative, t takes equally spaced values in $(0, 1)$.

A 2. $\{\varepsilon_t\}_{t \in \mathbb{Z}}$ is a strictly stationary and α -mixing process with mixing coefficients $\alpha(k)$, $E[\varepsilon_t] = 0$, $E|\varepsilon_t|^{2+\delta} < +\infty$, and $\sum_{k=1}^{+\infty} \alpha^{\delta/(2+\delta)}(k) < \infty$ for some $\delta > 2$.

A1 imposes a certain degree of smoothness for $s(t)$. This is because we want that the stochastic term absorbs transients while $s(t)$ mainly models long-term smooth variations and periodic behaviours. Since the SSW is not a noise component, but rather a structural component, we can’t restrict it to the usual linear process. The process $\{\varepsilon_t\}_{t \in \mathbb{Z}}$ has to accommodate transients, and it is well known that these have various time-decay structures during which either serial correlation vanishes at various speed, or non linear behaviours are introduced. Therefore the restrictions on $\{\varepsilon_t\}_{t \in \mathbb{Z}}$ cannot rule out serial correlation and non linearity. We instead assume that the sequence $\{\varepsilon_t\}_{t \in \mathbb{Z}}$ belongs to a fairly rich class of stochastic processes able to accommodate a wide class of features. We require that ε_t has fourth moment and that the series of mixing coefficients to the $\delta/(2 + \delta)$ exponent converges. Whereas the α -mixing assumption allows for various stochastic structures, the restrictions on the moments and mixing coefficients are needed for technical reasons. Nevertheless the existence of the fourth moment is not that strong in practice, because this would imply that the SSW has finite power variations, which is something that has to hold otherwise it would be impossible to record it.

Remark 1. The α -mixing assumption is new in this field. It is important to notice that there is some empirical evidence that, at least for some musical instruments, the stochastic term obtained after the application of a low-pass filter resembles 1/f-noise or similar fractal processes [see Voss and Clarke, 1978; Brillinger and Irizarry, 1998; Beran, 2004a]. However these results are based on periodgram analysis at fixed time window that treat the signal as if the processes involved were stationary and linear, which is questionable. The examples shown previously demonstrate that fixing a time scale for analyzing such data is problematic. Moreover Brillinger and Irizarry [1998] also shows empirical evidence of the departure of the stochastic component from linearity and Gaussianity. The α -mixing assumption allows to manage non linearity, departure from Gaussianity, and a certain

slowness in the decay of the dependence structure of the SSW. Certainly the α -mixing assumption would not be consistent with the long-memory nature of 1/f-noise. But again the 1/f-noise evidence depends on the time-scale adopted in the spectral domain.

Remark 2. Imagine we have a device that reduces the large energy swings. In signal processes such a device is called “dynamic compressor”. A compressor reduces the peakness of the sound energy especially at transients. Thus, estimating the power distribution of the stochastic part should reveal dynamic variations better than if we would look at observed samples.

4 Estimation

We want to obtain the distribution of the RMS power of the stochastic component. In order to do so we need to filter out the deterministic component $s(t)$ via non parametric methods. A natural candidate estimator is the Priestley-Chao kernel estimator [Priestley and Chao, 1972]

$$\hat{s}(t) = \frac{1}{nh} \sum_{i=1}^n K\left(\frac{t - i/n}{h}\right) y_i, \quad (4.1)$$

under the assumption

A 3. $K(\cdot)$ is a bounded and symmetric density function with compact support and bandwidth $h \in H = [c_1 n^{-1/5}; c_2 n^{-1/5}]$, where c_1 and c_2 are two positive constants such that c_1 is arbitrarily small while c_2 is arbitrarily large. Whenever $n \rightarrow \infty$ it happens that $nh \rightarrow \infty$.

Without loss of generality we will use the Epanechnikov kernel for its well known efficiency properties, but any other kernel function fulfilling A3 is welcome. Altman [1990] studied the kernel regression problem when the error term additive to the regression function exhibits serial correlation. Furthermore in the setup considered by Altman [1990] the error term is a linear process. The paper showed that when the stochastic term exhibits serial correlation, standard bandwidth optimality theory no longer applies. The author proposed an optimal bandwidth estimation which is based on a correction factor that assumes that the autocorrelation function is known. Therefore Altman’s theory does not apply here for two reasons: (i) in this paper the $\{\varepsilon_t\}_{t \in \mathbb{Z}}$ is not restricted to the class of linear processes; (ii) we do not assume that serial correlations are known. Let $\hat{\varepsilon}_t = y_t - \hat{s}(t)$, and let us define the cross-validation function

$$\text{CV}(h) = \left[1 - \frac{1}{nh} \sum_{j=-M}^M K\left(\frac{j}{nh}\right) \hat{\rho}(j) \right]^{-2} \frac{1}{n} \sum_{i=1}^n \hat{\varepsilon}_i^2; \quad (4.2)$$

where the first term is the correction factor à la Altman with the difference that it depends on the estimated autocorrelations of ε_t up to M th order. We show that the modification does not affect consistency at the optimal rate. The number of lags into the correction factor depends both on n and h . Intuitively consistency of the bandwidth selector can only be achieved if M increases at a rate smaller than nh , and in fact we will need the following technical requirement:

A 4. Whenever $n \rightarrow \infty$; then $M \rightarrow \infty$ and $M = O(\sqrt{nh})$.

This assumption is sufficient to estimate consistently the spectral density function in zero with respect to $\{\varepsilon_t\}_{t \in \mathbb{Z}}$. Note that such a condition makes clear the order of the parameter M with respect to the bandwidth h . The bandwidth is estimated by minimizing the cross-validation function, that is we set h at

$$\hat{h} = \operatorname{argmin}_{h \in H} \operatorname{CV}(h)$$

The next proposition relates \hat{h} to the optimal global bandwidth for which convergence rate is known. Let $\operatorname{MISE}(h; \hat{s})$ be the mean integrated square error of $\hat{s}(\cdot)$, and let h^* be the global minimizer of $\operatorname{MISE}(h; \hat{s})$. It is well known that the optimal global bandwidth h^* is of order $O(n^{-1/5})$.

Proposition 1. Assume A1, A2, A3 and A4. $\hat{h}/h^* \xrightarrow{p} 1$ as $n \rightarrow \infty$.

Remark 3. The previous result allows to apply (4.2) with $\hat{\rho}(j)$ under minimal conditions compared to Altman [1990] and Altman [1990]. In particular, the assumptions in Altman [1993] are stronger because the author has to estimate also the sample distribution of $\hat{\rho}(j)$. In the literature there are many papers on the bandwidth selection via cross-validation for kernel regression with dependent errors. For example, Hart [1991] is in the context of Altman [1990] but it requires some technical assumptions on the mixed moments of fourth order, and uses an objective function different from (4.2). Moreover, Xia and Li [2002] considers a non linear autoregressive stochastic process to estimate the bandwidth using the cross-validation for local polynomials estimators. In this paper the assumptions are very strong. In fact, the authors need that all moments are finite for the innovation process. Since we have only a deterministic signal in model (3.2), it is sufficient to use (4.2) as in Altman [1990] and our assumptions A1–A4 to derive a consistent estimator for the bandwidth by cross-validation.

The previous statement completes the smoothing part of our estimation procedure. Despite the dependence structure of ε_t we are able to estimate $s(\cdot)$ consistently with a bandwidth choice which attains the global optimal rate. A fair objection to this estimator is that the bandwidth is estimated globally. At first glance this is too restrictive because it has to be applied on time series such as those in Figure 1, however the reason why local bandwidth is not considered will be soon clear in the next section (see Remark 4). In analogy with equation (2.2) RMS power of the SSW is given by the sampling standard deviation of ε_t . Equation (2.2) only takes into account sum of squares, this is because theoretically PCM are always scaled to have zero mean. Notice that even though we assume that ε_t has zero expectation, we define RMS based on variances taking into account the fact that quantization could introduce an average offset in the PCM samples which would reflect into the sampling version of ε_t . Let us introduce the following quantities:

$$V_n = \frac{1}{n-1} \sum_{i=1}^n (\varepsilon_i - \bar{\varepsilon})^2, \quad \text{with} \quad \bar{\varepsilon} = \frac{1}{n} \sum_{i=1}^n \varepsilon_i. \quad (4.3)$$

The distribution of the RMS power of the SSW is given by the distribution of $\sqrt{V_n}$. By A2 it can be shown that $\sqrt{n}(V_n - \sigma_\varepsilon^2) \xrightarrow{d} \operatorname{Normal}(0, V)$, where $\sigma_\varepsilon^2 = \operatorname{E}[\varepsilon_t^2]$ and $V = \lim_{n \rightarrow \infty} n \operatorname{Var}[V_n]$. From now onward $G(\cdot)$ will denote the distribution function of a $\operatorname{Normal}(0, V)$.

Although the sequence $\{\varepsilon_i\}_{i \in \mathbb{Z}}$ is not observable, one can approximate the power distribution expressed by ε using its estimate. Replacing ε_i with $\hat{\varepsilon}_i$ in the previous formula we obtain:

$$\hat{V}_n = \frac{1}{n-1} \sum_{i=1}^n (\hat{\varepsilon}_i - \bar{\hat{\varepsilon}})^2, \quad \text{with} \quad \bar{\hat{\varepsilon}} = \frac{1}{n} \sum_{i=1}^n \hat{\varepsilon}_i.$$

The distribution of \hat{V}_n can now be used to approximate the distribution of V_n . One way to do this is to implement a subsampling scheme à la [Politis et al. \[2001\]](#). That is for all blocks of observations of length b (subsample size) one compute \hat{V}_n , in this case there would be $n - b + 1$ subsamples to explore. Then one hopes that the empirical distribution of the $n - b + 1$ subsample estimates of \hat{V}_n agrees with the distribution of V_n when both n and b grow large enough at a certain relative speed. This is essentially the subsampling scheme proposed by [Politis et al. \[2001\]](#), but it is of limited practical use here. A three minutes stereo song contains $n = 15,876,000$ samples, which means that one has to compute $\hat{s}(t)$ on such a long series. Even if this is in principle possible it would require a large computational power hardly achievable by regular computers. We solve the problem by introducing a variant to the subsampling scheme previously described. Namely instead of estimating $s(t)$ on the entire series, we estimate it on each subsample separately, then we use the average estimated error computed block-wise instead of $\bar{\hat{\varepsilon}}$ computed on the whole sample. Moreover a block-wise kernel estimate of $s(t)$ allows to work with the simpler global bandwidth instead of the more complex local bandwidth without losing too much in the smoothing step.

At a given time point t we consider a block of observations of length b and we consider the following statistics

$$V_{n,b,t} = \frac{1}{b-1} \sum_{i=t}^{t+b-1} (\varepsilon_i - \bar{\varepsilon}_{b,t})^2, \quad \text{and} \quad \hat{V}_{n,b,t} = \frac{1}{b-1} \sum_{i=t}^{t+b-1} (\hat{\varepsilon}_i - \bar{\hat{\varepsilon}}_{b,t})^2,$$

with $\bar{\varepsilon}_{b,t} = b^{-1} \sum_{i=t}^{t+b-1} \varepsilon_i$ and $\bar{\hat{\varepsilon}}_{b,t} = b^{-1} \sum_{i=t}^{t+b-1} \hat{\varepsilon}_i$. Notice that replacing $\bar{\hat{\varepsilon}}_{b,t}$ with $\bar{\hat{\varepsilon}}$ one has the subsampling scheme proposed in [Politis et al. \[2001\]](#). The empirical distribution functions of $V_{n,b,t}$ and $\hat{V}_{n,b,t}$ will be computed as

$$\begin{aligned} G_{n,b}(x) &= \frac{1}{n-b+1} \sum_{t=1}^{n-b+1} \mathbb{1} \left\{ \sqrt{b} (V_{n,b,t} - V_n) \leq x \right\}, \\ \hat{G}_{n,b}(x) &= \frac{1}{n-b+1} \sum_{t=1}^{n-b+1} \mathbb{1} \left\{ \sqrt{b} (\hat{V}_{n,b,t} - V_n) \leq x \right\}; \end{aligned}$$

where $\mathbb{1} \{A\}$ denotes the usual indicator function of the set A . We can state the following result:

Proposition 2. *Assume [A1](#), [A2](#), [A3](#) and [A4](#). Whenever $n \rightarrow \infty$, $b \rightarrow \infty$, $b/n \rightarrow 0$, then $\sup_x \left| \hat{G}_{n,b}(x) - G(x) \right| \xrightarrow{p} 0$.*

Furthermore the quantiles of the subsampling distribution also converges to the quantities of interest, that is those of V_n . This a consequence of the fact that $\sqrt{n}V_n$ converges weakly

to a Normal distribution, let it be F . Let define the empirical distributions:

$$F_{n,b}(x) = \frac{1}{n-b+1} \sum_{t=1}^{n-b+1} \mathbb{1} \left\{ \sqrt{b} V_{n,b,t} \leq x \right\},$$

$$\hat{F}_{n,b}(x) = \frac{1}{n-b+1} \sum_{t=1}^{n-b+1} \mathbb{1} \left\{ \sqrt{b} \hat{V}_{n,b,t} \leq x \right\}.$$

For $\gamma \in [0, 1]$ the quantities $q(\gamma)$, $q_{n,b}(\gamma)$ and $\hat{q}_{n,b}(\gamma)$ denote respectively the γ -quantiles with respect the distributions F , $F_{n,b}$ and $\hat{F}_{n,b}$. We adopt the usual definition that $q(\gamma) = \inf \{x : F(x) \geq \gamma\}$. The convergence result of the quantiles can now be stated.

Corollary 1. *Assume A1, A2, A3 and A4. Whenever $n \rightarrow \infty$, $b \rightarrow \infty$, $b/n \rightarrow 0$, then $\hat{q}_{n,b}(\gamma) \xrightarrow{p} q(\gamma)$ for any $\gamma \in [0, 1]$.*

However exploring all subsamples makes the procedure still computationally heavy. A second variant is to reduce the number of subsamples by introducing a random block selection. Let I_i , $i = 1, \dots, K$ be random variables indicating the initial point of every block of length b . We draw the sequence $\{I_i\}_{i=1}^K$, with or without replacement, from the set $I = \{1, 2, \dots, n-b+1\}$. The empirical distribution function of the subsampling variances of ε_t over the random blocks will be:

$$\tilde{G}_{n,b}(x) = \frac{1}{K} \sum_{i=1}^K \mathbb{1} \left\{ \sqrt{b} \left(\hat{V}_{n,b,I_i} - V_n \right) \leq x \right\},$$

and the next results states the consistency of \tilde{G} in approximating G .

Proposition 3. *Assume A1, A2, A3 and A4. Let $K \rightarrow \infty$, then $\sup_x \left| \tilde{G}_{n,b}(x) - G(x) \right| \xrightarrow{p} 0$.*

In analogy with what we have seen before we also establish consistency for the quantiles based on $\left\{ \hat{V}_{n,b,I_i} \right\}_{i=1}^K$. Let define the distribution function

$$\tilde{F}_{n,b}(x) = \frac{1}{K} \sum_{t=1}^K \mathbb{1} \left\{ \sqrt{b} \hat{V}_{n,b,I_t} \leq x \right\},$$

and let $\tilde{q}_{n,b}(\gamma)$ be the γ -quantile with respect to \tilde{F} .

Corollary 2. *Assume A1, A2, A3 and A4 and let $K \rightarrow \infty$, then $\tilde{q}_{n,b}(\gamma) \xrightarrow{p} q(\gamma)$.*

Hence the subsampling procedure proposed here consistently estimates the distribution of V_n and its quantiles. However, there is yet a limitation in the procedure, that is the fixed nature of the block length b . The reader could find hard to believe that in practice a fixed b can produce good results. For instance Figure 1 has been constructed so that there are two blocks of observation of equal size that have tremendously different structures. The question really is what would happen if a random block like the one in the top plot had been extracted. In principle one can think about estimating an optimal block size b , but again we have to accept that the astronomically large nature of n would take the

whole estimation time at Biblical scales. Notwithstanding these limitations, we propose a practical solution that is based on the intimate relation between the block length b and the optimal global bandwidth parameter \hat{h} . In fact, if a random block is large enough to contain piece of sounds with different dynamic structures, since the bandwidth across the block is taken fixed, the \hat{h} needs to become small enough to well fit the curve in the transition between two different dynamic stages. In those situations \hat{h} will approach the lower bound of H . What we do in practice is that we start from a given b , then if \hat{h} is equal to its lower bound we split the block into halves and we recompute \hat{h} on one of the two halves chosen at random, and if the new \hat{h} is still on the boundary we iterate the splitting up to the point when the estimated bandwidth is within H , or a maximum number r_{\max} of splits has been reached.

Remark 4. The splitting step is a practical solution to avoid estimation of b and/or the use of local bandwidth in the smoothing step. It can be easily seen that when splitting happens the resulting block length depends on \hat{h} and the consistency results stated previously do not account for it. However on real world sound waves splitting only happens on a small fraction of blocks for various reasonable values of b . Consistency theory for the estimated b is possible but would make the theoretical details too complex to be contained in this paper, whose focus is methodological rather than strictly theoretical. The choice of b still remains a crucial tuning but as we will see in Section 6, this can be done rather easily based on subject matter considerations.

5 Dynamic range statistic

The random nature of ε_t allows us to use statistical theory to estimate its distribution. If the SSW catches transient energy variations, then its distribution will highlight important information about the dynamic. The square root of \hat{V}_{n,b,I_i} is a consistent estimate of the RMS power of ε_t over the block starting from $t = I_i$. The loudness of the ε_t component over each block can be measured on the dBFS scale taking $L_{n,b,I_i} = -10 \log_{10} \hat{V}_{n,b,I_i}$. Notice that whenever we take continuous monotone transformations of \hat{V}_{n,b,I_i} , consistency for the quantities obtained through the subsampling is preserved.

In analogy with DRS (and its variants) we can define a DR measure based on the subsampling distribution of \hat{V}_{n,b,I_i} . We define the DR measure block-wise as $\text{DR}_{n,b,I_i} = -10 \log_{10} \hat{V}_{n,b,I_i}$. For a sound wave scaled onto the interval $[-1,1]$ this is actually a measure of DR of ε_t because it tells us how much the SSW is below the maximum attainable instantaneous power. We propose a measure of DR by taking the median of the subsampling distribution of DR_{n,b,I_i} , that is we define what we call “*Median Stochastic DR*” as

$$\text{MeSDR} = \text{med}_K \{ \text{DR}_{n,b,I_i} \quad i = 1, 2, \dots, K \},$$

where $\text{med}_K \{ \cdot \}$ denotes the empirical median over a set of K observations. Since DR_{n,b,I_i} is obtained by applying a monotone continuous transform to \hat{V}_{n,b,I_i} then consistency theory for the quantiles of DR_{n,b,I_i} applies. For waves scaled onto $[-1,1]$ it is easy to see that our statistic is expressed in dBFS. If the wave is not scaled onto $[-1,1]$, it suffices to add $20 \log_{10}(\text{maximum absolute observed sample})$, and this will correct for the existence of headroom.

The MeSDR has a nice practical interpretation. Suppose $\text{MeSDR}=20$, this means that 50% of the stochastic sound power is at least 10dBFS below the maximum instantaneous power. Hence large values of MeSDR indicates large dynamic swings. There are several advantages of such a measure. The DRS statistic is based on mean values which will be pushed toward the peak power it wants to compare. Contrary to what happens to DRS, the MeSDR is less influenced by the peaks. It can be argued that the SSW not only catches transients and non-periodic smooth components. In fact, it's likely the it fits noise, mainly quantization noise. This is certainly true, but quantization noise operates at extremely low levels and its power is constant over time. Moreover, since it is likely that digital operations producing DR compression (compressors, limiters, equalizers, etc.) increase the quantization noise (in theory this is not serially correlated), this would reflect in a decrease of MeSDR, so we should be able to detect DR compression better than classical DRS-like measures.

6 Empirical findings

6.1 Simulated compression

A common way of assessing a statistical procedure is to simulate data from a certain known stochastic process fixed as the reference truth, and then compute Monte Carlo expectations of bias and efficiency measures. The problem here is that writing down a stochastic model capable of reproducing the features of real-world music signal is too complex. Instead of trying to simulate such a complex signal we assess our methods based on artificial controlled experiments on real data. We considered two well recorded songs and we added various degrees of dynamic compression to assess whether our measure is able to highlight dynamic differences. A good method for estimating a measure of DR should consistently measure the loss of DR introduced by compressing the dynamic. In order to achieve a fair comparison we need songs on which little amount of digital processing has been applied. Chesky Records is a small label specialized in audiophile recordings, their “*Ultimate Demonstration Disc: Chesky Records’ Guide to Critical Listening*” (catalog number UD95), is almost a standard among audiophiles as test source for various aspects of hifi reproduction. We consider the left channel of tracks no.29, called “*Dynamic Test*”, and track no.17 called “*Visceral Impact*”. Both waveforms are reported in Figure 3. The “*Dynamic Test*” consists in a drum recorded near field played with an increasing level. Its sound power is so huge that a voice message warns against play backs at deliberately high volumes, which in fact could cause equipment and hearing damages. Most audiophiles subjectively consider this track as one of the most illustrious example of dynamic recording. The track is roughly one minute long. The “*Visceral Impact*” is actually the song “*Sweet Georgia Brown*” by Monty Alexander and elsewhere published in the Chesky catalog. The song has an energetic groove from the beginning to the end and it's about three minutes long. Differently from the previous track, that has increasing level of dynamic, this song has a uniform path. This can be clearly seen in Figure 3.

We removed initial and final silence from both tracks, and the final length (in sample units) for “*Dynamic Test*” is $n = 2,646,000$, while $n = 7,938,000$ for the second song. We then applied compression on both waves. A dynamic compressor is a function that

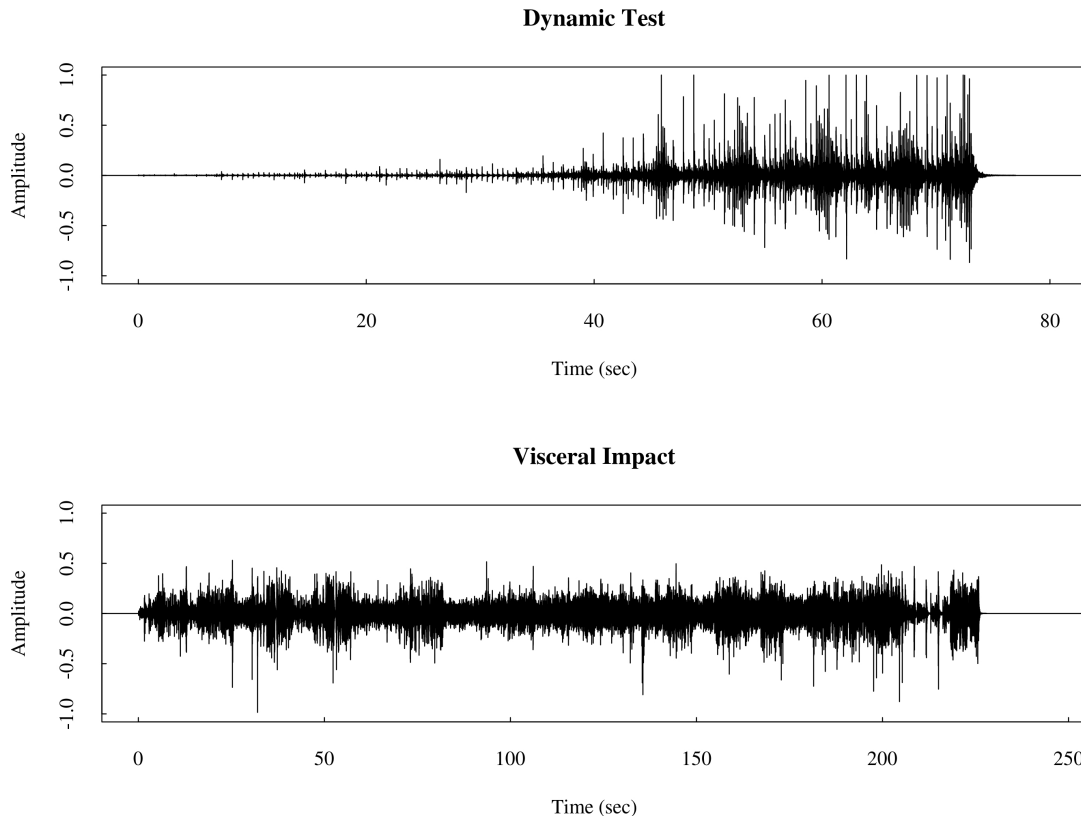


Figure 3: Waveforms of the left channel of the songs called “*Dynamic Test*” (track no.29) and “*Visceral Impact*” (track no.17) from the audiophile CD titled: “*Ultimate Demonstration Disc: Chesky Records’ Guide to Critical Listening*” by Chesky Record (catalog no. UD95).

whenever the original signal exceeds a given power (threshold parameter), the power of the output is scaled down by a certain factor (compression ratio parameter). From the statistical viewpoint this is similar to the well-known Box-Cox transform. Compression reduces the weight of tails of the power distribution, so that the distance between average signal level and peak level is reduced. This increases the perceived loudness, but when applied massively it destroys the music. We applied compression ratios from 1.5 to 5 with 0.5 increments, and in each case we compressed at threshold levels equal to -12dBFS and -24dBFS. With a threshold of -12dBFS and a compression ratio of 1.5, whenever the signal power is above -12dBFS, the compressor reduces the signal level to $2/3$ so that the input power is $1.5 \times (\text{output power})$. All this has been performed using SoX, an high quality audio digital processing software, with all other tuning parameters set at default values. For each wave we generated sixteen cases additional to the original wave. For each compressed version of the two waves we have computed our MeSDR statistics. The statistics are corrected for headroom so that they do not depend on it. In Figure 4 we report our results.

The subsampling algorithm has been run with several sets of input parameters to assess its stability. The results in Figure 4 are obtained with $K = 500$ for both songs, while $b = 2205$ (which means 50ms) for “*Dynamic Test*”, and $b = 3528$ (which means 80ms)

for “*Visceral Impact*”. A larger b for larger n obeys to the theoretical requirements that $b/n \rightarrow 0$ as n and b grow to ∞ . We also tried with larger values of b for both tracks but results did not change overall. Notice that while the theory is developed for fixed b , in practice we allow for smaller values of b by the splitting step (see Remark 4). In these cases the splitting never happened on more than 5% of subsamples. A 50ms block length for the second track would not have changed the results either. $K = 1000$ would not add too much to what we can find with $K = 500$. In Figure 4 we report a plot of MeSDR statistics with 95%-confidence bands based on the binomial distribution. Notice that we could have approximated the confidence bands for MeSDR with more precision by using the fact that $\sqrt{n}(V_n - \sigma_\varepsilon^2) \xrightarrow{d} \text{Normal}(0, V)$. However this requires further theoretical developments and space that do not add anything to the paper. In a comparison like this, one can choose to fix the seeds for all cases so that MeSDR is computed over the same subsamples in all cases. However this would not allow to assess the stability of the procedure against subsampling induced variance. The results presented here are obtained with different seeds for each case, but fixed seed has been tested and it did not change the main results. The constant M is fixed according to Proposition 1, i.e. $M = \lfloor \sqrt{n\hat{h}} \rfloor$.

First of all we notice that in all cases MeSDR can reproduce the somehow theoretical behaviour of DR vs compression ratios. If we had an input signal with constant unit RMS power, as the compression ratio increases DR should decrease at the speed of $\log_{10}(1/\text{compression ratio})$ for any threshold value. Of course, when the RMS power is not constant this is not true anymore but we expect a behaviour similar to the curve $y = \log_{10}(1/x)$ for $x > 0$. At both threshold levels for both songs the MeSDR does a remarkable discrimination between compression levels. For a given positive compression level none of the confidence bands for the -12dBFS threshold overlaps with the confidence bands for the -24dBFS case. For both songs the confidence intervals are larger for the -12dBFS case, and on average the “Dynamic Test” reports longer intervals. This is expected because increasing the threshold from -12dBFS to -24dBFS will increase the proportion of samples affected by compression so that the variations of MeSDR will be reduced. Moreover we also expect that if the dynamic of a song doesn’t have a sort of uniform path, as in the case of the “Dynamic Test”, the variability of the MeSDR will be larger. Summarizing, not only the level of MeSDR, but also its spread reveals important information on the DR.

It is worth to mention that DR measurement has become an hot topic in the audio business (an internet search about “*dynamic range compression*” produced more than two million results). As said before, perceived loudness can be digitally increased by compressing the DR. In 2008 the release of “*Death Magnetic*”, an album of the rock band Metallica, attracted medias’ attention for its extreme and aggressive loud sounding approach. Since then, the “*loudness war*” became of public domain outside the professional audio-world. The term “*war*” is used because conscious audio engineers and music lovers literally fight against such a practice. Compression is not reversible, once it is applied, the original dynamic is lost forever [see Katz, 2007; Vickers, 2010, and references therein]. The example above shows how MeSDR is able to detect consistently even small amount of compression.

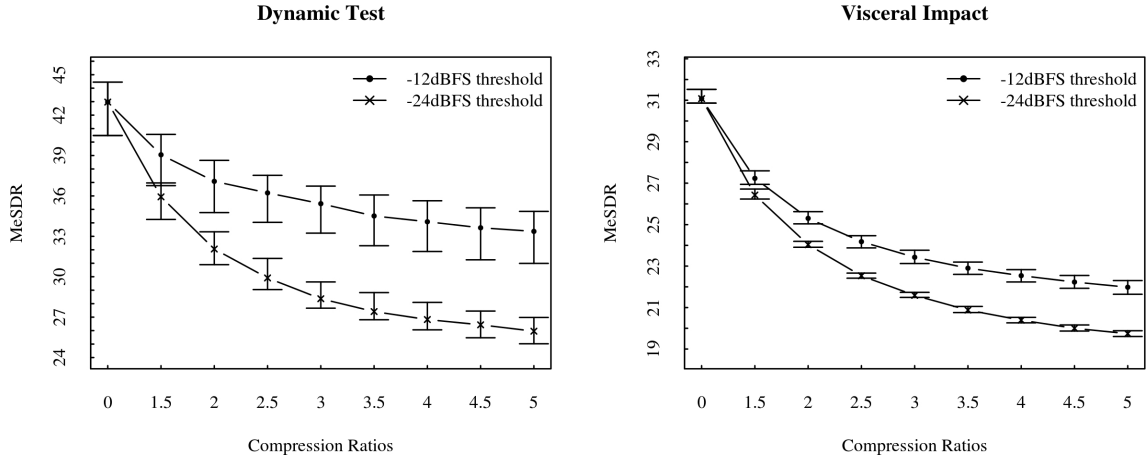


Figure 4: MeSDR statistics with 95%-confidence bands for the real-data simulation experiment.

6.2 Comparing different masterings

There are a number small record labels that gained success issuing remastered versions of famous albums. Some of this reissues are now out of catalogue and are traded at incredible prices on the second hand market. That means that music lovers actually price the value of the recording quality. On the other hand majors keep issuing new remastered versions promising miracles, they often claim the use of new super technologies termed with spectacular names. But many music lovers are very critical. Despite the marketing trend of mastering music with obscene levels of dynamic compression to make records sounding louder, human ears perceive dynamic compression better than it is thought. In this section we measure the DR of three different digital masterings of the song “In the Flesh?” from “*The Wall*” album by Pink Floyd. The album is considered one of the best rock recording of all times and “In the Flesh?” is a champion in dynamic, especially in the beginning (as reported in Figure 1) and at the end. We analysed three different masters: the MFSL by Mobile Fidelity Sound Lab (catalog UDCD 2-537, issued in 1990); EMI94 by EMI Records Ltd (catalog 8312432, issued in 1994); EMI01 produced by EMI Music Distribution (catalog 679182, issued in 2001). There are much more remasters of the album not considered here. The EMI01 has been marketed as a remaster with superior sound obtained with state of the art technology. The MFSL has been worked out by a company specialized in classic album remasters. The first impression is that the MFSL sounds softer than the EMI versions. However, there are Pink Floyd fans arguing that the MFSL sounds more dynamic, and overall is better than anything else. Also the difference between the EMI94 and EMI01 is often discussed on internet forums with fans arguing that EMI01 did not improved upon EMI94 as advertised.

We measured the MeSDR of the three tracks and compared the results. Since the large correlation between the two channels, we only measured the channel with the largest peak, that is the left one. The three waves have been time-aligned, and the initial and final silence has been trimmed. Since peaks are different, DR statistics have been adjusted for different headroom. The MeSDR has been computed with a block length of $b = 2205$ (that

Table 1: DR statistics for the left channel of “*In the Flesh?*” from “*The Wall*” album by Pink Floyd. “Lower” and “Upper” columns are limits of the 95%-confidence interval based on the asymptotic approximation of the distribution of the empirical quantiles.

Seed Number	Version	MeSDR	Lower	Upper
Equal	MFSL	29.767	29.222	30.377
	EMI94	25.995	25.401	26.687
	EMI01	25.963	25.375	26.640
Unequal	MFSL	29.551	29.268	30.257
	EMI94	25.808	25.484	26.448
	EMI01	25.628	25.197	26.198

is 50ms), and $K = 500$. We computed the MeSDR both with equal and unequal seeds across the three waves to test for subsampling induced variability when K is on the low side. Results are summarized in Table 1. First notice the seed changes the MeSDR only slightly. Increasing the value of K to 1000 would make this difference even smaller. The second thing to notice is that MeSDR reports almost no difference between EMI94 and EMI01. In a way the figure provided by the MeSDR is consistent with most subjective opinions that the MFSL, while sounding softer (probably due to a larger headroom), has more dynamic textures.

A further question is whether there are statistically significant differences between the sound power distributions of the tracks. It’s obvious that the descriptive nature of the approaches described in Section 2 cannot answer to such a question. Our subsampling approach can indeed answer to this kind of question by hypothesis testing. If the mixing coefficients of ε_t go to zero at a proper rate, one can take the loudness measurements $\{\text{DR}_{n,b,I_i} \quad i = 1, 2, \dots, K\}$ as almost asymptotically independent and then apply some standard tests for location shift. One can study an ad-hoc test for this problem. In this paper we simply apply an handy simple test like the Mann-Whitney. Using the set up with unequal seeds, we applied the Mann-Whitney test for the null hypothesis that the DR distribution of MFSL and EMI94 are not location-shifted, against the alternative that MFSL is right shifted with respect to EMI94. The resulting p-value $< 2.2 \times 10^{-16}$ suggests to reject the null at any sensible confidence level, and this confirms that MFSL sounds more dynamic compared to EMI94. Comparison between MFSL and EMI01 leads to a similar result. We also tested the null hypothesis DR distribution of EMI94 and EMI01 DR levels are not location-shifted, against the alternative that there is some shift different from zero. The resulting p-value=0.6797 suggests to not reject the null at any standard confidence level. The latter confirms the figure suggested by MeSDR that is there is no significant overall dynamic difference between the two masterings.

7 Concluding Remarks

Starting from the DR problem we exploited a novel methodology to estimate the variance distribution of a time series produced by a stochastic process additive to a smooth function

of time. The general set of assumptions on the error term makes the proposed model flexible and general enough to be applied under various situations not explored in this paper. The smoothing and the subsampling theory is developed for fixed global bandwidth and fixed subsample size. Optimal block size would be useful, but because of the typical large n , we proposed a splitting strategy that allows to vary the block lengths starting from a maximum. The study of the theoretical properties of the splitting will be the subject of another paper. We constructed a DR statistic that allows for inference. The advantage of our proposal is that it is based on the stochastic component. This has two main advantages: (i) technically speaking it allows to handle the sampling variations by means of inferential procedures; (ii) since power variations are about sharp changes in the energy levels, it is likely that these changes will affect the stochastic part of (3.2) more than the smooth component. In controlled experiment our DR statistic has been able to highlight consistently dynamic range compressions. Moreover we provided at least an example where the MeSDR statistic is able to reconstruct differences perceived subjectively on real music signals.

Appendix: proofs of statements

Proof of Proposition 1. First notice that A2–A3 in this paper imply that Assumptions A–E in Altman [1990] are fulfilled. In particular A2 on mixing coefficients of ε_t ensures that Assumptions E and D in Altman [1990] are satisfied. Let $\hat{\gamma}(j) = \frac{1}{n} \sum_{t=1}^{n-j} \hat{\varepsilon}_t \hat{\varepsilon}_{t+j}$ be the estimator of the autocovariance $\gamma(j)$ with $j = 0, 1, \dots$ and let us fix $r_n = \frac{1}{nh} + h^4$. First we note that by Markov inequality

$$\frac{1}{n} \sum_{i=1}^n (s(i/n) - \hat{s}(i/n))^2 \xrightarrow{P} \text{MISE}(\hat{s}; h) + o(r_n) \quad (.1)$$

Let us now rearrange $\hat{\gamma}(j)$ as

$$\begin{aligned} \hat{\gamma}(j) &= \frac{1}{n} \sum_{i=1}^{n-j} (s(i/n) - \hat{s}(i/n)) (s((i+j)/n) - \hat{s}((i+j)/n)) + \\ &+ \frac{1}{n} \sum_{i=1}^{n-j} (s((i+j)/n) - \hat{s}((i+j)/n)) \varepsilon_i + \\ &+ \frac{1}{n} \sum_{i=1}^{n-j} (s(i/n) - \hat{s}(i/n)) \varepsilon_{i+j} + \frac{1}{n} \sum_{i=1}^{n-j} \varepsilon_i \varepsilon_{i+j} \end{aligned}$$

By using (.1) and Schwartz inequality it results that $\hat{\gamma}(j) = \gamma(j) + O_p(r_n) + O_p(j/n)$, where the $O_p(j/n)$ is due to the bias of $\hat{\gamma}(j)$. It follows that also $\hat{\rho}(j) = \rho(j) + O_p(r_n) + O_p(j/n)$. Since $K(\cdot)$ is bounded from above then one can write

$$\frac{1}{nh} \sum_{j=-M}^M K\left(\frac{j}{nh}\right) \hat{\rho}(j) = \frac{1}{nh} \sum_{j=-M}^M K\left(\frac{j}{nh}\right) \rho(j) + \frac{M}{nh} O_p(r_n) + \frac{M^2}{n} O_p\left(\frac{1}{nh}\right);$$

and by A4 it holds true that

$$\frac{1}{nh} \sum_{j=-M}^M K\left(\frac{j}{nh}\right) \hat{\rho}(j) = \frac{1}{nh} \sum_{j=-M}^M K\left(\frac{j}{nh}\right) \rho(j) + o_p(r_n).$$

By expression (14) in Altman [1990] plus Markov inequality we have that

$$\text{CV}(h) - \text{MISE}(\hat{s}; h) = o_p(r_n).$$

By the same arguments as in the proof of Theorem 1 in Chu and Marron [1991], it follows that \hat{h} , the minimizer of $\text{CV}(h)$, is equal to h^* , the minimizer of $\text{MISE}(\hat{s}; h)$, asymptotically in probability. \square

Proof of Proposition 2. First notice that under A2 conditions of Theorem 4.1 in Politis et al. [2001] hold. Let us denote $r_n = \frac{1}{nh} + h^4$, which by Proposition 1 is $r_n = \left(\frac{1}{n}\right)^{\frac{4}{5}}$ at the optimal h . Along the same lines of Proposition 1 we can write

$$\frac{1}{b} \sum_{t=1}^b (\hat{\varepsilon}_t - \varepsilon_t)^2 = O_p(r_n) + O(1/b).$$

The order $O(1/b)$ happens because $|U_b(i/b) - U(x)| = O(1/b)$, where $U_b(\cdot)$ and $U(\cdot)$ are the empirical and true distribution functions, respectively, for the uniform random variable in $(0, 1)$. Now $\sqrt{b}r_n \rightarrow 0$ as $n \rightarrow \infty$, and it follows that $\sqrt{b}(\hat{V}_{n,b,t} - V_{n,b,t}) \xrightarrow{P} 0$. Then, we can conclude that $\sqrt{b}(\hat{V}_{n,b,t} - V_n)$ has the same asymptotic distribution as $\sqrt{b}(V_{n,b,t} - V_n)$. Let us denote $Z_{1t} = \sqrt{b}(V_{n,b,t} - V_n)$ and $Z_{2t} = \sqrt{b}(\hat{V}_{n,b,t} - V_{n,b,t})$, hence

$$\hat{G}_{n,b}(x) = \frac{1}{n-b+1} \sum_{t=1}^{n-b+1} \mathbb{1}\{Z_{1t} + Z_{2t} \leq x\}.$$

By the same arguments used for the proof of Slutsky theorem the previous equation can be written as

$$\begin{aligned} \sup_x \left| \hat{G}_{n,b}(x) - G(x) \right| &\leq \sup_x |G_{n,b}(x \pm \xi) - G(x)| + \\ &+ \frac{1}{n-b+1} \sum_{t=1}^{n-b+1} \mathbb{1}\{|Z_{2t}| > \delta\} \end{aligned}$$

for any positive constant ξ . Since $G(x)$ is continuous at any x it follows that $\sup_x |G_{n,b}(x) - G(x)| \xrightarrow{P} 0$ by Theorem (4.1) in Politis et al. [2001]. Moreover by A2 $Z_{2t} \xrightarrow{P} 0$, for all t and thus

$$\frac{1}{n-b+1} \sum_{t=1}^{n-b+1} \mathbb{1}\{|Z_{2t}| > \xi\} \xrightarrow{P} 0,$$

for all $\xi > 0$, which proves the result. \square

Proof of Corollary 1. Using the same arguments as in Proposition 1 we have that $\hat{F}_{n,b}(x) - F_{n,b}(x) = o_p(1)$. By the continuity of $F(x)$ at all x we have that $q_{n,b}(\gamma) \xrightarrow{P} q(\gamma)$ by Theorem 5.1 in Politis et al. [2001]. Therefore $\hat{q}_{n,b}(\gamma) \xrightarrow{P} q(\gamma)$. \square

Proof of Proposition 3. Let $P^*(X)$ and $E^*(X)$ be the conditional probability and the conditional expectation of a random variable X with respect to a set $\chi = \{Y_1, \dots, Y_n\}$. Applying the Markov inequality to the measure P^* we have that

$$P^* \left(\tilde{G}_{n,b}(x) \geq \xi \right) \leq \frac{1}{\xi} E^* \left(\tilde{G}_{n,b}(x) \right)$$

for any constant $\xi > 0$. But $P(I_i \in I) = \frac{1}{n-b+1}$ for all $i = 1, 2, \dots, n-b+1$. Therefore

$$E^* \left(\tilde{G}_{n,b}(x) \right) = \frac{1}{n-b+1} \sum_{t=1}^{n-b+1} \mathbb{1}\left\{ \sqrt{b} \left(\hat{V}_{n,b,I_i} - V_n \right) \leq x \right\} = \hat{G}_{n,b}(x).$$

By Proposition 1 $\hat{G}_{n,b}(x) \xrightarrow{P} G(x)$ for all x , and thus $\tilde{G}_{n,b}(x) - G(x) \xrightarrow{P} 0$ at any x . The proof is completed by using the same arguments as in the proof of Theorem 2.1 (ii) in Politis et al. [2001]. \square

Proof of Corollary 2. It follows the proof of Corollary 1 by replacing Proposition 1 with Proposition 2. □

References

- Altman, N. S. (1990). Kernel smoothing of data with correlated errors. *Journal of the American Statistical Association* 85(411), 749–759.
- Altman, N. S. (1993). Estimating error correlation in nonparametric regression. *Statistics & probability letters* 18(3), 213–218.
- Ballou, G. (2005). *Handbook for Sound Engineers*. Focal Press.
- Bennett, W. R. (1948). Spectra of quantized signals. *Bell Syst. Tech. J* 27(3), 446–472.
- Benson, D. (2004). *Mathematics and music*. University of Georgia. Department of Mathematics.
- Beran, J. (2004a). Music-chaos, fractals, and information. *Chance* 17(4), 7–16.
- Beran, J. (2004b). *Statistics in musicology*, Volume 12. CRC Press.
- Boley, J., M. Lester, and C. Danner (2010). Measuring dynamics: Comparing and contrasting algorithms for the computation of dynamic range. In *Proceedings of the AES 129th Convention, San Francisco*.
- Brillinger, D. R. and R. A. Irizarry (1998). An investigation of the second-and higher-order spectra of music. *Signal Processing* 65(2), 161–179.
- Chu, C. K. and J. S. Marron (1991). Comparison of two bandwidth selectors with dependent errors. *The Annals of Statistics*, 1906–1918.
- Crocker, M. J. (1998). *Handbook of Acoustics*. Wiley-Interscience.
- Hart, J. D. (1991). Kernel regression estimation with time series errors. *Journal of the Royal Statistical Society. Series B (Methodological)*, 173–187.
- Irizarry, R. A. (2001). Local harmonic estimation in musical sound signals. *Journal of the American Statistical Association* 96(454), 357–367.
- Katz, B. (2007). *Mastering audio: the art and the science*. Focal Press.
- Perez-Alcazar, P. R. and A. Santos (2002). Relationship between sampling rate and quantization noise. In *14th International Conference on Digital Signal Processing*, Volume 2, pp. 807–810. IEEE.
- Politis, D. N. and J. P. Romano (1994). Large sample confidence regions based on subsamples under minimal assumptions. *The Annals of Statistics* 22(4), 2031–2050.
- Politis, D. N., J. P. Romano, and M. Wolf (2001). On the asymptotic theory of subsampling. *Statistica Sinica* 11(4), 1105–1124.
- Priestley, M. B. and M. T. Chao (1972). Nonparametric function fitting. *Journal of the Royal Statistical Society* 34, 385–392.

- Risset, J. C. and M. V. Mathews (1969). Analysis of musical-instrument tones. *Physics today* 22, 23.
- Thomson, D. J. (1982). Spectrum estimation and harmonic analysis. *Proceedings of the IEEE* 70(9), 1055–1096.
- Vickers, E. (2010). The loudness war: Background, speculation and recommendations. In *Proceedings of the AES 129th Convention, San Francisco, CA*, pp. 4–7.
- von Helmholtz, H. (1885). *On the sensations of tone (English translation A.J. Ellis)*. New York: Dover.
- Voss, R. F. and J. Clarke (1978). "1/f noise" in music: Music from 1/f noise. *The Journal of the Acoustical Society of America* 63, 258.
- Xia, Y. and W. Li (2002). Asymptotic behavior of bandwidth selected by the cross-validation method for local polynomial fitting. *Journal of multivariate analysis* 83(2), 265–287.